JOURNAL OF PROPULSION AND POWER
Vol. 17, No. 5, September–October 2001

Acoustic-Wave/Blade-Row Interactions Establish Boundary Conditions for Unsteady Inlet Flows

Miklos Sajben* and Hazem Said†
University of Cincinnati, Cincinnati, Ohio 45221

Reliable computation of unsteady flows in high-speed airbreathing inlets requires that the outflow boundary condition applied at the compressor face provide a reasonable simulation of the compressor behavior. Traditional boundary conditions, for example, constant pressure or constant velocity, disagree with experimental observations. A one-dimensional, linearized theory is offerred to predict transients induced by downstream-moving acoustic waves arriving at a single row of stationary or moving blades. The results include acoustic reflection and transmission coefficients and also a coefficient describing the strength of the induced vorticity wave. The knowledge of the acoustic reflection coefficient allows formulation of the outflow boundary condition at the compressor face for a time-accurate analysis of the inlet flow. The analysis considers the effects of inflow Mach number, flow angles upstream/downstream of the blade row, and the blade height change across the blade row. The coefficients are given as simple algebraic expressions applicable to both stationary and rotating rows. The reflective behavior of a fixed geometry blade row is illustrated throughout its performance map. The reflection coefficients vary between wide limits, suggesting that the use of correct outflow conditions is essential to the realistic, time-accurate prediction of unsteady inlet flows.

Nomenclature

$\boldsymbol{A}_{\pm}$	=	wave coefficients for acoustic waves resulting from transient
a	=	speed of sound
b	=	passage height (radial dimension)
C_x	=	axial chord
c	=	absolute value of gas velocity in stationary coordinates
$\boldsymbol{G}$	=	generating wave (initiating the transient)
M	=	Mach number
N	=	compressor rotational speed, rpm
p	=	absolute static pressure
r_m	=	mean radius of blade annulus
S	=	blade passage area normal to velocity vector
s	=	tangential spacing of blades
T	=	absolute static temperature
U	=	absolute value of the blade velocity
$\tilde{U}$	=	blade speed normalized by $\hat{a}_{tu}$
$\boldsymbol{V}$	=	wave coefficient for vorticity wave produced in transient
W	=	mass flow per blade passage, or mass flow for engine in Sec. V.B.
w	=	absolute value of gas velocity in blade coordinates
x, y, z	=	axial, tangential, and radial coordinates
α	=	flow angle with respect to axial direction, in stationary coordinates
β	=	flow angle with respect to axial direction, in blade coordinates
β_0	=	blade angle at leading or trailing edge, with respect to axial direction
γ	=	ratio of specific heats, 1.4 for air
Δ	=	difference of properties across a wave
$\Delta\beta$	=	flow deflection angle across blade row, positive for compressors, $\beta_u - \beta_d$
δ_d	=	deviation angle, $\beta_d - \beta_{0d}$
δ_u	=	incidence angle, $\beta_u - \beta_{0u}$
ζ	=	total pressure loss coefficient
η	=	adiabatic efficiency of blade row
λ	=	ratio of densities downstream and upstream of blade row
μ	=	ratio of static pressures downstream and upstream of blade row
ρ	=	density
σ	=	ratio of passage heights downstream and upstream of blade row
τ	=	duration of incident acoustic wave
χ	=	ratio of temperatures downstream and upstream of blade row
ω	=	vorticity

Subscripts

corr	=	corrected quantities (in compressor performance maps)
f	=	final value, after transient is completed
is	=	isentropic process
ref	=	reference (standard sea level) conditions (pressure, temperature)
t	=	total (stagnation) value
u, d	=	undisturbed flow property upstream and downstream of blade row, respectively
x, y, z	=	x, y, z component of vector
$1, 2, \ldots, 6$	=	regions in x–t diagram

Superscripts

$'$	=	disturbance quantity
$\hat{}$	=	quantity in stationary coordinates
$\star$	=	sonic value

Received 22 November 2000; revision received 8 March 2001; accepted for publication 9 March 2001.

*Professor Emeritus, Department of Aerospace Engineering and Engineering Mechanics, College of Engineering, P.O. Box 210070. Fellow AIAA.

†Graduate Student, Department of Aerospace Engineering and Engineering Mechanics, College of Engineering, P.O. Box 210070.

I. Introduction

UNSTEADY inlet flow computations represent a significant part of designing supersonic airbreathing propulsion systems and their controls. The design must evaluate the inlet response to all controllable parameters that affect its operation, and it must also

ensure that the system is stable in response to accidentally occurring unsteady processes (such as flying through atmospheric disturbances).

During any transient operation, the inlet and the compressor dynamically interact with each other, and the conditions at the interface are determined jointly by the two components. A downstream propagating pressure (acoustic) disturbance interacting with a compressor stage typically induces pressure disturbances propagating both upstream and downstream, and it also creates convective disturbances. The full simulation of this response requires that the computation of transient events simultaneously include both the inlet and the compressor. Unfortunately, unsteady computations including both components are extremely complex, costly, and so far have been performed only as research projects. In engineering development projects, the cost and time constraints usually dictate that these computations be performed on isolated inlets. In this approach the inlet computations require a compressor face boundary condition (CFBC), the role of which is to provide the best possible approximation to the compressor behavior.

Until quite recently, no experimental evidence has been available that could have guided the formulation of such boundary conditions. For want of any guidance, numerical computations resorted to extending the well-established steady-state boundary conditions to unsteady situations. Conditions of constant pressure, constant velocity, constant Mach number, zero streamwise gradient, a virtual choked nozzle, etc., have been applied, despite the complete lack of experimental or even theoretical justification for any of them.

The crudeness of these traditional outflow boundary conditions is in strong contrast with the high sophistication of the codes they are combined with. Unfortunately, the validity of the results is determined by the weakest link, and the outcome of even the most advanced, unsteady viscous code is subject to the large uncertainties introduced by the outflow boundary condition. A series of studies dealt with this issue,[1–7] all of which indicate that the effect of the outflow condition on the results is major, and the resulting uncertainties represent a significant risk to the design of supersonic aircraft. The presently common ad hoc outflow boundary conditions are clearly in need of revision.

The present study is linearized, that is, the flow is thought of as a known steady flow onto which small-amplitude unsteady disturbances are superimposed. On a fundamental level, disturbances can be classified into three types: acoustic, vorticity, and entropy. If the flow is uniform and parallel (which is a reasonable first approximation for the flow near a compressor face), then these disturbances are independent of each other, and their effects are linearly superimposed.[8] Acoustic disturbances are capable of propagating both upstream and downstream at the speed of sound relative to the gas. Vorticity and entropy disturbances are convected downstream at the flow speed. When any one of these disturbances reaches the compressor face, a transient is initiated that gives rise to two new acoustic waves (one in each direction) and also a vorticity and an entropy wave. [It is a question of semantics whether the convected disturbances (vorticity and entropy) can be considered waves. The usage of the term is widespread and will be adopted here for simplicity.] These four waves will be referred to as product waves. Of these, only the upstream acoustic wave is capable of propagating into and affecting the inlet. The problem of characterizing the compressor face as a boundary condition thus amounts to properly representing the upstream-moving acoustic wave generated when a disturbance of some type reaches the engine. All disturbance types are capable of producing upstream-moving acoustic waves. The mechanisms are different for each case, and the complete solution of the problem will ultimately require the prediction of all three types of transients.

Estimates show that in the context of the inlet/compressor interface, reflections of acoustic disturbances dominate those induced by entropy and vorticity disturbances. Accordingly, we discuss only transients initiated by the arrival of acoustic disturbances from upstream.

The two acoustic product disturbances are commonly characterized in terms of reflection and transmission coefficients, which are basically dimensionless ratios of the respective resultant/incident disturbance amplitudes, both taken at the same location and same instant. Reflection and transmission coefficients are simply and uniquely related to acoustic impedance, which is a well-established concept in acoustics and is commonly used to state boundary conditions in acoustic problems. Similar coefficients can be defined for the resulting entropy and vorticity disturbances. The four coefficients will be given the collective name wave coefficients.

II. Previous Related Efforts and Present Scope

A. Analytical Studies

Useful and relevant information is available from several theoretical efforts dealing with engine noise, due to Kaji and Okazaki,[9,10] Mani and Horvay,[11] and Amiet.[12] These investigators treated the propagation of blade-generated noise from the interior of the engine to the outside. They have derived complex reflection and transmission coefficients for planar, harmonic, acoustic waves obliquely incident on two-dimensional blade rows. The applicability of these results to the CFBC problem was not raised in the cited papers.

Cumpsty and Marble[13] investigated noise propagation from combustors through the turbine and paid special attention to entropy waves, which could have large amplitudes when the fluctuating temperature exhaust is strongly deflected by turbine blades.

More recent analytical investigations were carried out by Paynter et al.[14] and Paynter,[15] who presented a simple one-dimensional analysis for the computation of the reflection coefficient for acoustic step changes[14] and also for incident vorticity disturbances.[15]

Past interest was focused on harmonic waves, but the first experiments squarely addressing the CFBC problem were accomplished using short-duration pulses (see Sec. II.C). The behavior of pulses was not well understood at the time, which necessitated theoretical work to establish their proper characterization and to clarify the relationship between pulse data and classical reflection coefficients.[16–18] This effort led to simple algebraic formulas for the product waves created by acoustic pulses passing through two-dimensional blade rows.

B. Computational Studies

In the early 1990s computer codes reached the level of sophistication required for a reliable investigation of inlet dynamics. Studies by Mayer and Paynter,[6] Cole,[1] Clark,[7] Chung,[2] and Chung and Cole[3] have clearly shown that the outflow boundary condition plays a very important role in determining the solution and that traditional CFBCs allow a wide variation in the properties of the predicted inlet flows, depending on which is chosen.

In search of clarification of the related fundamental issues, Paynter carried out a number of unsteady Euler computations to explore the processes induced by acoustic, vorticity, and entropy waves incident on a linear cascade of flat plates.[15,19] He also presented a method for implementing outflow boundary conditions in numerical codes, making use of a given value of a reflection coefficient 1 (Paynter[14] and Paynter et al.[15]).

Suresh et al.[20] and Suresh and Cole[21] combined inlet and engine codes (LAPIN, NPARC, ADPAC, and DYNTECC) to represent both components simultaneously in simulating the arrival of various waves to blade rows. They made numerous comparisons to available experimental data.

C. Experimental Studies

Peacock[22] and Das[23] reported on experiments with inlet/compressor systems, using periodic excitation in the inlet by mechanical methods and including measurements of interstage pressures within the compressor. The properties of the inlet oscillations measured in these experiments were affected not only by the compressor face conditions, but also by the entire inlet configuration and boundary conditions at the front end of the inlet. In part due to this complexity and in part due to the different focus of the authors, neither paper led to a characterization of the compressor face in a manner that would be useful for analytical or computational fluid dynamics studies.

More recent experimental work on this problem began at the University of Cincinnati in 1993. Preliminary studies have shown that periodic disturbances generate such a proliferation of reflected/transmitted waves, that it is impossible to isolate the reflection of the incident wave from unwanted reflections coming from elsewhere in the system, or from background compressor noise.[24,25] The work, therefore, focused on transients induced by short-duration, high-intensity acoustic pulses arriving to the engine from upstream. Such pulses and the product waves created by them are easily recognized and tracked even in very noisy environments. The project yielded the first set of experimental data specifically intended to shed light on the boundary condition issue[26–29] and has provided significant insight into the subject.

D. Scope of Present Work

With the exception of relatively recent NASA work, the cited analytical and computational investigations assumed two-dimensional flow and computed the product wave coefficients as functions of two-dimensional blade row properties. Effects of blade loading (flow deflection across the blade row) has received limited attention only. Changes in blade height in the axial direction were not considered in any previous work.

The present paper offers an approximate, linearized theory for the calculation of wave coefficients that includes the effects of (1) flow direction change across the blades, (2) blade height change across the blade row, (3) tangential blade motion, (4) viscous losses in the undisturbed flow, and (5) nonzero incidence and deviation angles. The description is one dimensional, implying planar disturbances normal to the axis. The approach Mach number extends up to unity, that is, supersonic approach flow is not included.

III. Undisturbed Steady Flow

A. Problem Definition

Steady flow through the blade rows of an axial-flow compressor is a classical problem, and many methods and commercial software are available for its determination. Any one of these may be used. However, the present theory is approximate, and it is not economical to expend much effort to obtain a sophisticated mean flow solution. The simple one-dimensional theory described in this section is both adequate and compatible with the method of unsteady analysis presented.

We consider the steady, adiabatic flow of a compressible, perfect gas through a stationary, linear cascade of blades with zero thickness (Fig. 1). The blade shape is not specified in detail, only the inlet and exit angles are given. The flow may or may not be aligned with the blade angles at either the inlet or the exit, that is, nonzero incidence and deviation angles are permitted as inputs from any external source.

The height of the flow passage, that is, the blade height, within the cascade is allowed to vary. The passages leading to and away from the cascade are both assumed to have constant heights, but the heights of the inlet and exit passages are not necessarily the same. Because of the combination of the flow angle and height changes, the cross-sectional areas of a passage (measured normal to the velocity vector) are generally different on the two sides.

The region of interest extends to infinity in the $\pm x$ directions and is periodic in the y direction with a period equal to the blade spacing s. The flow is described in terms of passage averages taken over planes normal to the x axis and is effectively one dimensional, with x being the only independent space variable. The linear blade row is intended to be an approximate description of annular blade assemblies found in turbomachinery, and the terms axial and tangential will be freely used to designate the x and y directions.

The Mach number on the upstream side is assumed to be at most sonic. If the approach flow is supersonic, the nature of the reflection/transmission process is drastically different and will be treated in a separate paper. Viscous losses will be taken into account by specifying a total pressure loss coefficient across the blade row. This coefficient is treated as an empirical input to the present theory.

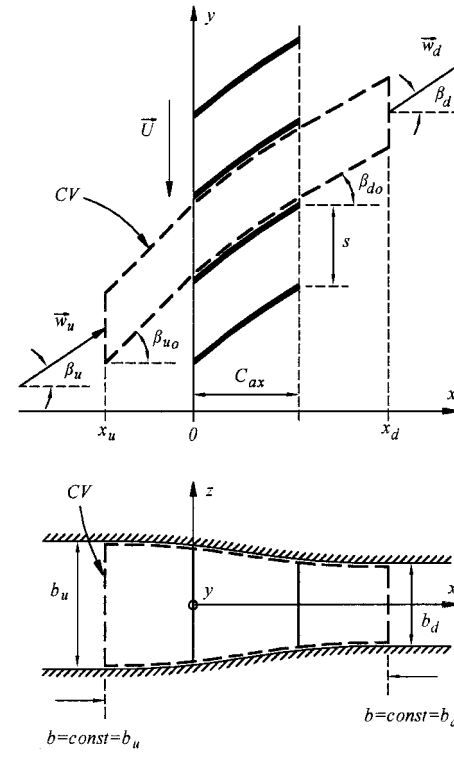

Fig. 1 Blade row configuration.

B. Undisturbed Flow in a Stationary Blade Row

We define a three-dimensional control volume [(CV) Fig. 1] that contains all of the fluid within a finite axial length of a single blade passage of a linear cascade. Outside the blade row, the CV is separated from adjacent blade passages by planes that are tangential to the blades at the leading and trailing edges. The flow is to the right, such that the directions right and left are synonymous to downstream and upstream. The upstream and downstream boundaries of the CV are planes normal to the x axis, each plane being located in a constant-height passage. In the radial direction, the CV boundaries coincide with the solid walls of the hub and the casing.

The flat plane boundaries extending from the leading and trailing edges are usually not streamlines, and fluid may pass through them. However, in the integral equations of motion, the mass flux, normal and tangential stress, and enthalpy flux contributions from these two walls cancel out, due to the assumed periodicity in the y direction. As a result, the problem may be viewed as a one-dimensional, compressible duct flow with a streamwise variable area. The standard one-dimensional gasdynamic equations apply, provided the appropriate velocities, Mach numbers, and cross-sectional areas are used. In particular, the velocity to be used is that along the streamwise direction and is given in terms of the vector components as follows:

$$w = w_x/\cos\beta, \qquad M = M_x/\cos\beta \tag{1}$$

The area to be used is that normal to the flow direction. The area and the area ratio appropriate for a one-dimensional description then are

$$S = sb\cos\beta, \qquad \frac{S_d}{S_u} = \frac{sb_\alpha \cos\beta_d}{sb_u\cos\beta_u} = \sigma\frac{\cos\beta_d}{\cos\beta_u} \tag{2}$$

It is noted that for compressors the blade height is either constant or decreases axially, and, therefore, σ is equal to or less than one. However, due to the reduction of flow angle from the leading to the trailing edge, the ratio S_d/S_u is greater than one, that is, the passage diverges, thereby creating the desired static pressure rise.

The mass flow at any axial station can be expressed as (see any gasdynamics textbook):

$$W = \gamma[2/(\gamma+1)]^{\frac{1}{2}[(\gamma+1)/(\gamma-1)]}\, p_t S^*/a_t \tag{3}$$

In this expression, the local values of p_t and a_t must be used. S^* is the local sonic area, defined by the actual local cross-sectional area and the local Mach number through the well-known relationship

$$S/S^* \equiv f(M) = (1/M)([2/(\gamma+1)] \times \{1 + [(\gamma-1)/2]M^2\})^{\frac{1}{2}[(\gamma+1)/(\gamma-1)]} \quad (4)$$

Equation (3) can be applied to either side of the cascade. Because the mass flow and the stagnation temperature is the same on both sides, we have

$$p_{tu} S_u^* = p_{td} S_d^* \quad (5)$$

This expression can be manipulated to introduce the ratio of the actual and sonic areas

$$S_d / S_d^* = S_d / S_u (p_{td}/p_{tu}) S_u / S_u^* \quad (6)$$

A total pressure loss coefficient is defined as

$$\zeta = (p_{tu} - p_{td})/(p_{tu} - p_u) \quad (7)$$

Using the loss coefficient definition of Eq. (7), the ratio of downstream/upstream total pressures can be expressed in terms of known input quantities, as follows:

$$\mu_t = p_{td}/p_{tu} = 1 - \zeta(1 - p_u/p_{tu}) = 1 - \zeta\left(1 - \left\{1 + [(\gamma-1)/2]M_u^2\right\}^{-\gamma/(\gamma-1)}\right) \quad (8)$$

When the function f defined by Eq.(4) is used, Eq.(6) can be written as

$$f(M_d) = (\sigma \mu_t \cos\beta_d / \cos\beta_u) f(M_{ux} / \cos\beta_u) \quad (9)$$

Knowing the downstream flow angle β_d, one can determine M_d from Eq. (9) by a root-finding procedure. If information is available on the deviation angle, then the actual downstream flow angle can be used, otherwise one may use the exit blade angle as an approximation. [Note that the function $f(M)$ has a minimum at $M = 1$, such that a specified value of f can be attained at two Mach numbers, one being subsonic and the other supersonic. Only the subsonic values are used here]. The axial component, M_{dx} readily follows from Eq. (1). Having obtained M_d, ratios of static flow properties can be readily computed. Some ratios that will be needed later are

$$\chi \equiv \frac{T_d}{T_u} = \frac{1 + [(\gamma-1)/2]M_u^2}{1 + [(\gamma-1)/2]M_d^2} \quad (10)$$

$$\mu \equiv p_d/p_u = \mu_t \chi^{\gamma/(\gamma-1)} \quad (11)$$

$$\lambda \equiv \rho_d/\rho_u = \mu/\chi \quad (12)$$

C. Undisturbed Flow in a Moving Blade Row

We assume that the upstream flow properties are specified in the stationary coordinate system, that is, the velocity components c_{xu} and c_{yu} are given (as is usually the case), along with the thermodynamic state of the gas flowing into the CV. The blade speed with respect to the stationary coordinate system will be specified here in a normalized form:

$$\tilde{U} = U/\hat{a}_{tu} \quad (13)$$

The connection between velocities seen in the stationary and moving frames is illustrated by the velocity triangle in Fig. 2. Note that the blade movement is in the negative y direction, that is, $U_y = -U$ and $U_x = 0$.

The flow is unsteady in the stationary frame, but is steady in a coordinate system attached to the blades. Transformation to a coordinate system moving with the blades does not alter any of the static flow properties, nor the axial velocity components, but the tangential velocity components do change. The velocity in the blade frame is defined by the following relations:

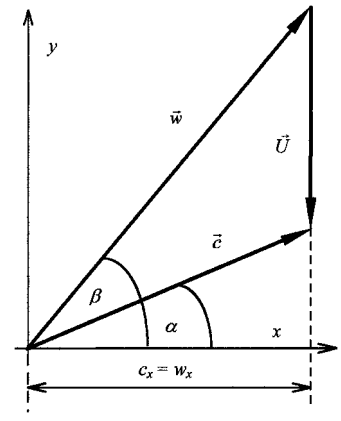

Fig. 2 Velocity triangle connecting stationary and blade-frame velocity vectors.

$$w_x = w\cos\beta = c_x = c\cos\alpha \quad (14a)$$

$$w_y = w\sin\beta = c_y + U = c\sin\alpha + U \quad (14b)$$

Equations (14) determine the upstream velocity vector in the blade coordinates, which then allows the execution of the solution procedure described in Sec. III.B. The solution yields the blade-frame Mach numbers on both sides of the cascade. When Eqs. (14) are used to retransform velocities into the stationary frame, the Mach numbers in the stationary frame are readily obtained.

The ratios of total pressures and total temperatures across the blade row (in the stationary frame) are the primary descriptors of compressor performance. In possession of the stationary frame Mach numbers, and using the ratios of static properties [Eqs. (10) and (11)], they are calculated as follows:

$$\hat{\chi}_t \equiv \frac{\hat{T}_{td}}{\hat{T}_{tu}} = \chi \frac{1 + [(\gamma-1)/2]\hat{M}_d^2}{1 + [(\gamma-1)/2]\hat{M}_u^2} \quad (15)$$

$$\hat{\mu}_t \equiv \hat{p}_{td}/\hat{p}_{tu} = \mu(\chi_t/\chi)^{\gamma/(\gamma-1)} \quad (16)$$

The adiabatic compressor efficiency is given conventionally by

$$\eta = \frac{\hat{T}_{td,is} - \hat{T}_{tu}}{\hat{T}_{td} - \hat{T}_{tu}} = \frac{\hat{\mu}_t^{(\gamma-1)/\gamma} - 1}{\hat{\chi}_t - 1} \quad (17)$$

where $\hat{T}_{td,is}$ is the exit total temperature that would be reached by isentropic compression from $\hat{p}_{tu}$ to $\hat{p}_{td}$. The efficiency is readily calculated from the results of Eqs. (15) and (16).

IV. Unsteady Disturbance Flow

A. Problem Definition

The transient wave/cascade interaction process considered here is superimposed on the known steady flow. A planar acoustic disturbance arrives at the cascade from upstream, the plane of the wave being normal to the x axis. The disturbance is an isentropic change in fluid properties, characterized only by its magnitude, defined as the difference between the final and initial values of static pressure. The magnitudes are sufficiently small to allow linearization with respect to the undisturbed flow. The change occurs during some short time interval τ, but the detailed time history of the change is arbitrary and is not considered. If $\tau = 0$ then the disturbance is a simple step change.

The disturbance is expected to generate two acoustic waves (one reflected upstream and one transmitted downstream), plus one vorticity and one entropy wave. It is assumed that the product wave structures are comparable to the generating wave, that is, they all represent a change from one level to another within a short time interval, the interval being comparable to τ. The spatial and temporal details of the interaction or of the product waves are not considered. The goal is to determine the product wave magnitudes after

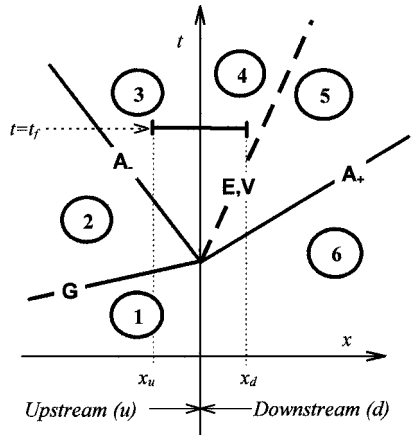

Fig. 3 Distance–time diagram indicating wave trajectories.

the interaction is completed and steady flow has been reestablished within the cascade passages.

Figure 3 shows the process as an x–t diagram. Figure 3 shows the waves and the blade row as single lines, but it is understood that each has a finite spatial extent. The x-velocity component of a right-moving acoustic waves is $w_x + a$ and that of a left-moving wave is $w_x - a$. The vorticity and entropy waves move at the axial flow speed w_{dx}. The initial wave is labeled ***G*** (generating), and the product waves are labeled $\boldsymbol{A}_-$, $\boldsymbol{A}_+$, ***V***, and ***E***, respectively. The flow properties are assumed to be constant over each of the regions numbered 1–6.

B. Characterization of Waves

1. Acoustic Waves

Small-amplitude acoustic waves are governed by the linear wave equation. In a constant-area duct, they propagate at the speed of sound with respect to the gas, without distortion. Thermodynamic properties are governed by the isentropic relations throughout the flow at any instant. In particular, density perturbations at any location are given by

$$\rho' = p'/a^2 \tag{18}$$

It can be readily shown using the momentum and continuity equations that the velocity and pressure changes on the two sides of an acoustic wave are connected by

$$\Delta w_x' = \pm(\Delta p'/\rho a) \tag{19}$$

where the $+$ and $-$ signs apply to right- and left-moving waves, respectively.

2. Vorticity Wave

Because we consider x as the only independent space variable, the only nonzero vorticity component is axial and is given by

$$\omega_z = \frac{\partial w_y}{\partial x} \tag{20}$$

A vorticity wave is, thus, defined in this study as a region where the tangential component of the velocity changes with x. The genesis of such a wave in the acoustic-wave/cascade interaction is explained in physical terms as follows.

Consider a cascade flow at design conditions, where the incident flow is aligned with the leading edge and the exhaust flow is aligned with the trailing edge. Consider a transient induced by a right-moving, acoustic, compression step change incident on this cascade (***G***). Figure 4 shows an instantaneous snapshot of the streamline pattern after the transient is completed, at time t_f. Wave ***G*** does not affect the y velocity component anywhere, but increases the axial velocity [cf. Eq. (19)] such that the inlet flow angle is reduced ($\beta_2 < \beta_u$). If the chord/spacing ratio is greater than about 1.5, then we can assume that the exit flow remains aligned with the blade.[12] The temporal change of flow deflection across the blades reduces

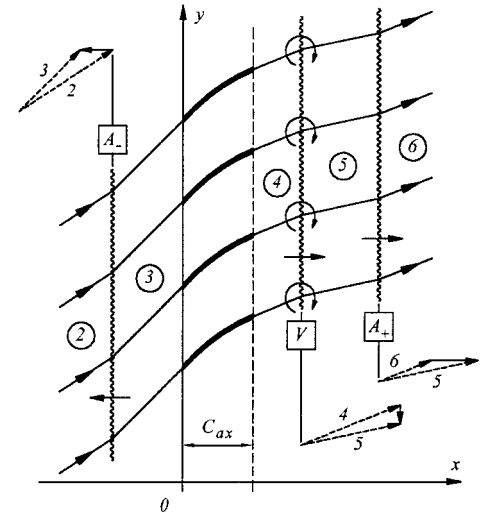

Fig. 4 Instantaneous streamline pattern after transient is completed; small-velocity triangles illustrate details of abrupt flow direction changes at waves.

the tangential blade force (~lift), which generates a starting vortex from every blade. The vortices in this case rotate clockwise and convect away from the cascade at the flow velocity w_{dx}. Figure 4 shows the resulting vertical row of vortices at time t_f, after which steady flow has been reestablished within the cascade.

A row of vortices with identical signs can be idealized into a vertical slip line. A slip line is characterized by a discontinuity of the velocity component parallel to the slip line, while the normal component remains continuous. This slip line constitutes the vorticity wave ***V***.

There is no change of pressure or axial velocity across the vorticity wave. This can be understood if one views the wave in a coordinate system moving in the x direction at speed w_{dx}. Because the discontinuity in w_{dy} is convected at the mean flow velocity, an observer in this system would see two parallel streams (regions 4 and 5) moving in the y direction, the one within region 4 having a higher velocity. In this moving system, there is no streamline curvature and no acceleration; therefore, the pressure and the axial velocity are common over regions 4 and 5. Because the disturbance flow is inviscid, the temperature and density disturbances do not change across the vorticity wave either. We may write

$$\Delta p' = 0 \tag{21a}$$

$$\Delta w_x' = 0 \tag{21b}$$

$$\Delta \rho' = 0 \tag{21c}$$

$$\Delta T' = 0 \tag{21d}$$

However,

$$\Delta w_y' \neq 0 \tag{22}$$

The offered physical argument involving starting vortices is believed to be new. This view provides an explanation for the zigzag pattern illustrated in Fig. 4, with streamline direction changes occurring at waves ***V*** and $\boldsymbol{A}_+$. The same streamline patterns also appear in the Euler computations of Paynter et al.[14] The present theory, conforming to the stated ideas, predicts details of the computed patterns quite accurately.[17]

3. Entropy Wave

If the transient process includes viscous phenomena, then an entropy wave is also generated. Given some characterization of the total pressure loss or drag associated with the disturbance, it is possible to calculate the magnitude of the entropy disturbance and the corresponding wave coefficient. The resulting complications in the theoretical description are considerable. Because viscous effects are

believed to play only a limited role in the incident-wave/cascade interaction, we will assume that the entire transient process is inviscid. As a result, the magnitude of the entropy wave is zero, and we will not be concerned with it further.

C. Disturbance Flow for a Stationary Blade Row

We again focus on the state of the flow that exists at some time t_f, after the product waves moved away from the cascade and steady state has been reestablished within the CV of Fig. 1. At this instant, the product waves are still in motion, but they are outside the CV. Within the CV, the flow differs slightly from the undisturbed state, but it is steady, and the problem is solvable by the application of steady-state conservation equations to the CV.

Referring to Fig. 3, the flow is undisturbed over regions 1 and 6, that is, all disturbance properties there are zero. The disturbance properties in region 2 are given as part of the problem specification, and the magnitude of pressure change here, p'_2, will be used to normalize the magnitudes of the product waves. There are three different regions with unknown properties, (regions 3, 4, and 5). The disturbance flow is fully defined in each region by four quantities, p', ρ', w'_x, and w'_y, such that a full solution amounts to the determination of 12 unknowns.

We can apply the steady-state, linearized conservation equations for mass and energy to the CV. Because the flow angles in regions 3 and 4 differ from those in the undisturbed flow, there is flow across the planar CV boundaries that separate adjacent passage streams outside the blade row. However, as was the case in the mean flow computations, the influx/outflux terms and the surface stress integrals over these boundary segments exactly cancel due to the assumed periodicity, and the equations need only to consider the original inflow and outflow surfaces (at left and right). Omitting details, the conservation equations for the CV can be written as follows.

Continuity:

$$\rho_u w'_{3x} + \rho'_3 w_{ux} = (\rho_d w'_{4x} + \rho'_4 w_{dx})\sigma \tag{23}$$

Energy:

$$(p'_3/\rho_u) + w_{ux} w'_{3x} + w_{uy} w'_{3y} = (p'_4/\rho_d) + w_{dx} w'_{4x} + w_{dy} w'_{4y} \tag{24}$$

One more important relation is obtained by assuming that the direction of the exit velocity disturbance is the same as the undisturbed flow direction:

$$w'_{4y} = w'_{4x} \tan\beta_d \tag{25}$$

The isentropic relations between ρ' and p' [Eq. (18)] can be applied to eliminate the density disturbances in regions 3 and 4. The tangential velocity is unchanged across acoustic waves, hence, the equation

$$\Delta w'_y = 0 \tag{26}$$

can be also applied to each acoustic wave on the upstream side, leading to the elimination of w'_{3y}. Equation (25) is used to eliminate w'_{4y} from Eq. 24. Equation (19) can be used to eliminate all axial velocity disturbances in favor of pressure disturbances. There is one vorticity wave present, and across this wave we can apply Eq. (21a), eliminating p'_4. Eventually Eqs. (23–25) contain only p'_2, p'_3, p'_5 and w'_{4y}. We use p'_2 as a reference quantity to define the desired dimensionless wave coefficients describing the amplitudes of the two product acoustic waves and the vorticity wave, which reduces the number of unknowns to three. The number of equations and number of unknowns are then matched, thereby making the problem solvable. Omitting details, the results are

$$\boldsymbol{A}_- \equiv \frac{p'_3 - p'_2}{p'_2} = \left(\frac{1+M_{ux}}{1-M_{ux}}\right) \times \left[\frac{\left(1-\sigma\lambda\Big/\sqrt{\chi}\right)(1+M_{dx}) + M_{dx}\tan^2\beta_d}{\left(1+\sigma\lambda\Big/\sqrt{\chi}\right)(1+M_{dx}) + M_{dx}\tan^2\beta_d}\right] \tag{27}$$

$$\boldsymbol{A}_+ \equiv \frac{p'_5}{p'_2} = \frac{2\lambda(1+M_{ux})}{\left(1+\sigma\lambda\Big/\sqrt{\chi}\right)(1+M_{dx}) + M_{dx}\tan^2\beta_d} \tag{28}$$

$$\boldsymbol{V} \equiv \frac{\rho_u a_u w'_{4y}}{p'_2} = \frac{\left(2\Big/\sqrt{\chi}\right)(1+M_{ux})\tan\beta_d}{\left(1+\sigma\lambda\Big/\sqrt{\chi}\right)(1+M_{dx}) + M_{dx}\tan^2\beta_d} \tag{29}$$

Note that the values of M_{dx}, χ, and λ (the undisturbed temperature and density ratios across the cascade) depend on all of the input parameters (σ, β_u, β_d, M_u, and ζ) and, therefore, the effects of the input parameters on the wave coefficients are much more complex than what the explicitly indicated dependencies seem to imply.

D. Disturbance Flow for a Moving Blade Row

The formulation of this problem for a stationary row in stationary coordinates is identical to the problem for a moving row stated in moving coordinates. It follows that the solution applies to both cases: the wave coefficients are determined by the undisturbed flowfield as seen in the coordinate system attached to the blades, regardless of the tangential speed the blade row may have.

However, this does not mean that rotation does not have an effect on the wave coefficients. If the upstream flow conditions are fixed in the stationary frame and the tangential speed of the blade row is varied, then the incidence angles and the entire flowfield in the blade frame will vary and, therefore, so will the wave coefficients. The nature of this variation will be explored in Sec. V.B.

V. Discussion of Results

The number of independent parameters affecting the wave coefficients is quite large, and this paper is by necessity limited to the illustration of the effects of a few selected parameter combinations. In particular, results on transmission and vorticity induction coefficients will not be discussed in detail.

A. Reflection Coefficients

1. *Area change*

To separate the effects of area variation from those due to incoming swirl and flow deflections, we set $\beta_u = \beta_d = 0$. This implies that the velocities are purely axial and no forces are present due to blades. Only subsonic approach flows are of interest.

It is easy to see that this set of parameters describes flow in a very simple system consisting of two constant (but unequal) area duct segments, aligned along the same axis and joined by an arbitrarily shaped transition segment. The acoustic wave is approaching the area change from upstream and is being reflected from it. Because the tangential velocity component is zero, there is no vorticity wave, the process is purely acoustic, and Eq. (29) is irrelevant. The reflection coefficient of Eq. (27) simplifies to

$$\boldsymbol{A}_- = \left(\frac{1+M_u}{1-M_u}\right)\left[\frac{1-\sigma\lambda\Big/\sqrt{\chi}}{1+\sigma\lambda\Big/\sqrt{\chi}}\right] \tag{30}$$

The required density and temperature ratios are easily calculated with one-dimensional gasdynamics equations. Results are given in Fig. 5 for $\zeta = 1$, isentropic flow.

Figure 5 shows that a converging duct ($\sigma < 1$) has a positive reflection coefficient, while an area enlargement has a negative one. A compression wave will produce a compressive reflection from an area reduction and an expansive reflection from an area enlargement. The magnitude of the reflection increases with deviation of the area ratio from unity. The effect of the Mach number is to increase the magnitude of the reflection coefficient, for any value of the area ratio. The increase is quite significant. It is easily shown that for the low-speed limit of $M_u = 0$, the reflection coefficient simplifies to

$$\boldsymbol{A}_- = (1-\sigma)/(1+\sigma) \tag{31}$$

This expression is identical with the classical acoustics result for an area change in a duct with stationary air, on the limit of long wavelengths.[30]

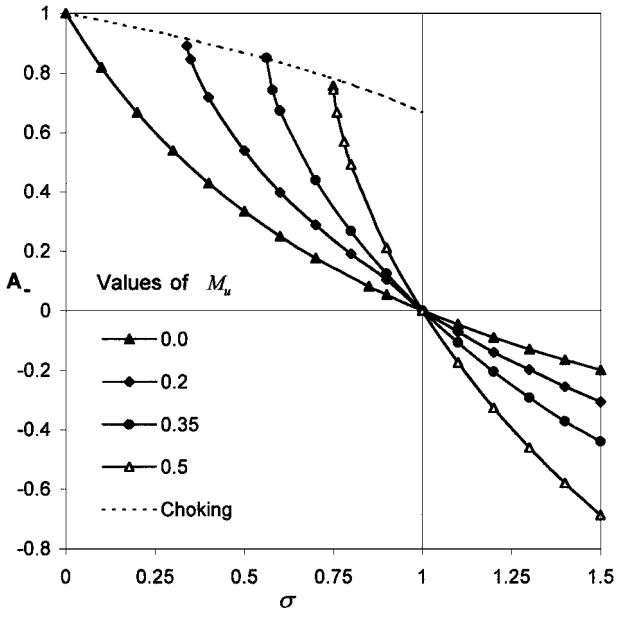

Fig. 5 Reflection coefficient vs area change, with upstream Mach number as parameter.

There is no aerodynamic limit on area enlargement, but area reduction is limited by choking for any given initial Mach number. Figure 5 includes a dashed line showing the choking boundary. The equation expressing this dashed line can be obtained from Eq. (27), by setting $M_d = 1$ and similarly simplifying the expressions for χ and λ [Eqs. (10) and (12)]. After some algebra, the reflection coefficient for choked area reductions is

$$(A_-)^* = \frac{1 - [(\gamma - 1)/2]M_u}{1 + [(\gamma - 1)/2]M_u} \tag{32}$$

[Note that Eq. (32) has been also obtained by Rogers[31] using a different approach.]

For airflow, the reflection coefficient for a choked duct end is never less than $2/3 = 0.667$, that is, choking is always a strongly reflecting, hard termination. Note that simulated choked nozzles have been used as CFBCs in the past. Because the actual reflection coefficient at moderate Mach numbers tends to be small compared to unity, the choked nozzle CFBC is likely to be a poor choice for subsonic compressors.

2. *Axial Mach Number and Upstream Flow Angle*

Figure 6 shows the variation of the reflection coefficient with upstream axial Mach number, for unloaded, two-dimensional flat plate cascades. It is evident that increasing Mach number and increasing blade angles both increase the reflection coefficient. The blade angle effect is quite reasonable because larger angles represent larger blade surfaces normal to the flow direction. If the axial Mach number M_{ux} is increased while keeping β_u constant, then M_u will become equal to one when M_{ux} reaches the value of $\cos\beta_u$. The present theory is not applicable beyond this limit, and all curves are terminated. At the point of termination, the reflection coefficient is unity for all blade angles (this is true for unloaded flat plates only, not for other parameter combinations).

3. *Upstream Flow Angle and Flow Deflection*

Figure 7 shows the effect of upstream flow angles on the reflection coefficient, for several given values of flow deflection $\Delta\beta$, which is a measure of blade loading. The variation shown is the net results of two opposing influences. Increasing deflection angle increases the streamtube divergence [cf. Eq. (2)], which would lead to an increasingly negative reflection coefficient if occurred in isolation (cf. Fig. 5). Increasing upstream flow angle, on the other hand, tends to increase the reflection coefficient. The net result is that

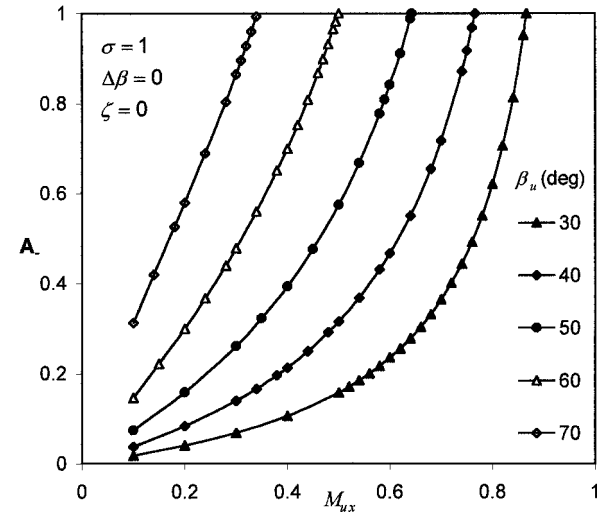

Fig. 6 Reflection coefficient vs upstream axial Mach number, with upstream flow angle as parameter.

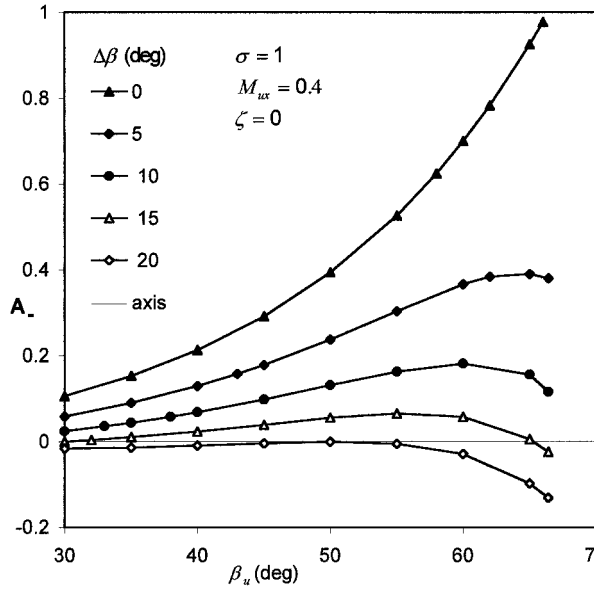

Fig. 7 Reflection coefficient vs upstream flow angle, with flow deflection as parameter.

the reflection coefficient values are lower than those for a flat plate cascade. Note that even negative reflection coefficients are possible if the deflection is sufficiently large.

4. *Passage Height Change and Upstream Flow Angle*

Figure 8 shows the effects of passage height changes on the reflection coefficient for fixed M_{ux} and fixed deflection angle, for several values of the upstream flow angle. As could be expected from the individual effects illustrated in Figs. 5 and 6, the reflection coefficient increases with β_u and decreases with σ. Considering the variable ranges typical to operational compressors, the effect of blade height change is quite significant. Ten degrees of change in β_u has about as much effect on A_- as a change of 0.05 in σ.

5. *Loss Coefficient*

Detailed investigation of the results (omitted for brevity) showed that increasing total pressure losses in the undisturbed flow will increase the reflection coefficient. The effect is relatively modest, especially considering that ζ is likely to vary only by small amounts among competing design alternatives.

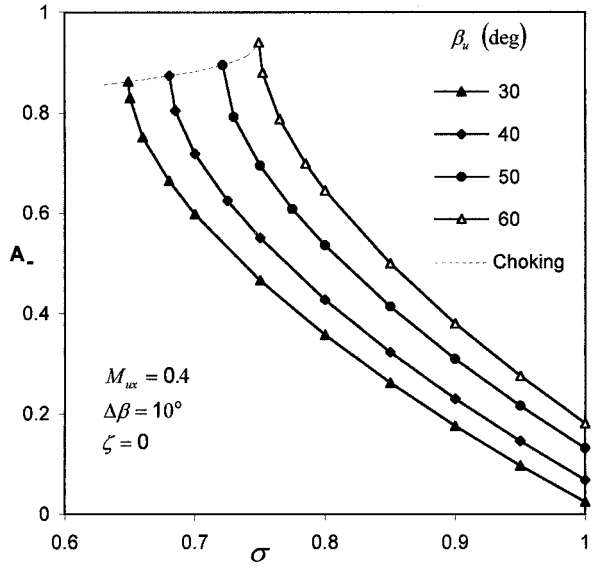

Fig. 8 Reflection coefficient vs area ratio, with upstream flow angle as parameter.

B. Compressor Performance Map

In Figs. 5–8 each point represents a separate realization of the geometry and flow parameter combination, that is, they are design charts in which the geometry is considered to be freely variable. It is of interest to examine off-design behavior also, that is, investigate how the reflection coefficient varies when the operational conditions of a given compressor are changed. This representation illustrates the effects of the concurrent variation of a number of basic parameters, as it occurs in an actual compressor.

A convenient approach is to superimpose lines of constant reflection coefficient on a standard compressor performance map. The ordinate of this chart is the ratio of exit-to-inlet total pressures, both as measured in the stationary coordinate system. The horizontal axis and the parameter of the curves shown in the chart are as follows.

Corrected mass flow:

$$W_{\text{corr}} \equiv \frac{W\sqrt{\hat{T}_{tu}/T_{\text{ref}}}}{(\hat{p}_{tu}/p_{\text{ref}})} \tag{33}$$

Corrected speed:

$$N_{\text{corr}} \equiv \frac{N}{\sqrt{\hat{T}_{tu}/T_{\text{ref}}}} \tag{34}$$

The corrected speed is directly related to the normalized blade speed $\tilde{U}$ used in this analysis. After specifying a representative (mean) radius of the annular flow passage upstream of the blade row, we have

$$N_{\text{corr}} = (60/2\pi)(a_{\text{ref}}/r_{\text{mu}})\tilde{U} \tag{35}$$

For illustration, a single-stage research compressor developed by NASA has been selected. Detailed description of the compressor and the results of extensive performance testing are available.[32] Tables 1 and 2 contain the principal geometrical parameters. The report includes data both for the rotor separately and for the stage as a rotor/stator combination. We used only rotor data taken at the mean radius. The loss coefficients and deviation angles (which are inputs required by the present theory) were obtained by interpolation, using simple curve fits to data. The performance map was computed using the undisturbed flow calculation method of Sec. III and is shown in Fig. 9. The pressure ratio is overpredicted by about 10–25%, which is not unexpected because the calculation completely neglects all end effects in the blade passage. In all other respects, the calculation well duplicates the measured trends and magnitudes. Because the current use of the results is limited to the illustration of reflection coefficient variations under operational conditions, the calculation method is adequate.

Table 1 Information on compressor used for illustration (Ref. 32)

	Axial location[a]	
Parameter	*u*	*d*
Tip radius, m	0.254	0.254
Hub radius, m	0.2032	
	0.2032	
Annulus area, m^2	0.07297	
	0.07297	
Blade angle, deg	61.08	39.45
Blade height ratio	1.000	
Flow angle, deg	62.4	45.4

[a]Locations *u* and *d* are defined by the available data at the midradius leading and trailing edges.

Table 2 Performance parameters at design point

Parameter	Value
W_{corr}, kg/s	9.457
N_{corr}, rpm	9,170
$\hat{p}_{td}/\hat{p}_{tu}$	1.328

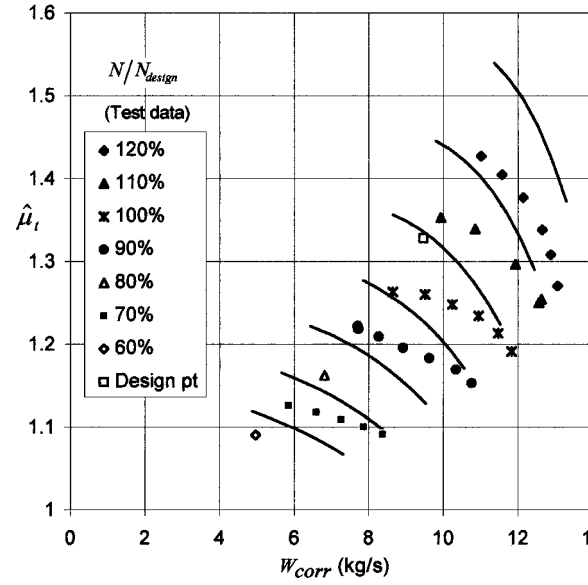

Fig. 9 Performance map for the subsonic compressor of Ref. 32, comparing data (symbols) with the calculation method of Sec. III (solid lines).

Figure 10 shows the (calculated) performance map with contours of constant A_- values superimposed. Figure 10 shows that the reflection coefficient increases with increasing mass flow and decreases with increasing pressure ratio. The reflection coefficient values range from 0.06 to 0.18, that is, a threefold change occurs over the operating envelope. In comparison, constant velocity and constant pressure boundary conditions imply values of $+1$ and -1, respectively. Obviously, neither one comes close to being correct, and the constant pressure condition misses even the sign.

C. Comparisons to Results from Other Sources

The present results reduce to previously published expressions applicable to unloaded, two-dimensional, flat plate cascades with inviscid undisturbed flow.[17,18] Analytical results for flat plate cascades are also available from other investigators,[12,14] which have been used for comparison in an earlier publication.[17] Very good agreement was found in all cases.

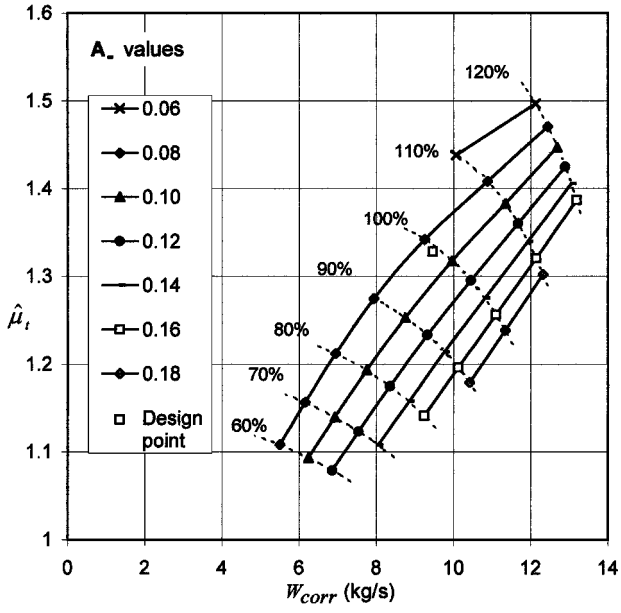

Fig. 10 Performance map for the subsonic compressor of Ref. 32; solid lines are contours of constant reflection coefficients.

Unfortunately, there appear to be no experimental data either for linear or annular cascades, or for single rotors, that could be compared with the present results. The most relevant data set is a University of Cincinnati experiment mentioned earlier,[29] but this work employed a 10-stage compressor (21 blade rows) at low subsonic speeds. Multiple reflections involving the first four or five stages were clearly evident in the results, leading to significantly higher reflection coefficients than those predicted for a single blade row.

VI. Incorporating Results in Computer Codes

The implementation of reflection coefficients as boundary conditions into a computer code is a separate and very significant challenge that is not addressed in this paper. It is believed that there may be a variety of ways to accomplish this, and that the method selected would significantly depend on the structure of the code. The results of this paper would be appropriate for use with a variety of implementation procedures.

One method, proposed originally by Paynter, has been incorporated into the widely used WIND code by Slater and Paynter.[33] The formulation accounts for the response to both acoustic and convective disturbances arriving from upstream. The reflection coefficients are required inputs as functions of the radius over the outflow boundary. Slater and Paynter's implementation is included in the version 4 official WIND release.

VII. Comments

The present paper provides approximate answers to a class of situations of practical interest. Open questions remain, some of which will be discussed.

A. Other Generating Waves

The present theory postulates a downstream-moving acoustic wave as the generating disturbance. There are practical situations in which the generating disturbance could be any one of the other three types of waves. The method presented here can be extended to these cases without much difficulty.

B. Multistage Compressors

If the compressor has many stages, then the transmitted portions of the disturbance travel to later stages and get reflected from them. The reflections will cross the compressor face in the upstream direction with some time delay after the first reflection produced by the first blade row. Because there are many such internal reflections, the overall reflection is no longer a simple mirror image of the incident wave, rather it is stretched out in time. If the streamwise length of the stretched-out reflection is comparable to the length of the inlet, then the present approach to posing CFBCs will become inadequate and multistage effects will have to be accounted for.

Cumpsty and Marble[13] developed a method of determining reflections and transmissions generated by a multirow turbomachine, upon the arrival of an incident wave of any type. The calculation requires the complete characterization of all individual rows, including all four wave coefficients for each. Unfortunately, the method is limited to two-dimensional configurations. An extension of the method to variable blade heights would be welcome.

C. Analogous Problems in Other Technologies

The need for appropriate inflow or outflow boundary conditions also arises in the computational simulation of dynamic processes in combustors, nozzles, and afterburners. These components are also bounded by a turbomachine either at their inflow or outflow boundary, or at both. The representation of rotating machines by simple boundary conditions thus poses the same kind of challenge for the modelers of combustors and nozzles as the one faced by inlet engineers. The present study could probably be extended to deal with such analogous problems.

VIII. Summary

Approximate analytical formulas have been presented to compute the acoustic reflection coefficient for a single row of stationary or moving blades. Knowledge of this coefficient permits the formulation of a realistic boundary condition for the compressor face that properly describes the dynamic behavior of the compressor. The boundary conditions so defined represent a major improvement over the ad hoc boundary conditions traditionally used in the computation of unsteady inlet flows. Their use in propulsion practice should lead to improved reliability in inlet stability assessment and control system design.

The theory accounts for the effects of approach Mach number, upstream and downstream flow angles, blade height change across the blade row, and also for viscous losses in the undisturbed flow. The approach Mach number is limited to subsonic values.

In the few simple cases where a comparison could be made to other theories, the agreement is very good. There are no directly comparable experimental data available.

The results show that the reflection coefficient can vary widely, from low negative numbers up to unity, depending on the combination of parameters characterizing the situation. The results also show that two-dimensional theories ignore the important effects of the blade height change and should not be relied on when the annulus area changes significantly across the blade row. The wide range of possible values strongly suggests that the use of proper downstream boundary conditions is indispensable for the accurate prediction of unsteady inlet flows.

Acknowledgments

The first author is deeply indebted to Gerald Paynter (The Boeing Company) and to Gary Cole (NASA John H. Glenn Research Center at Lewis Field; now retired) for countless discussions on the subject and for providing valuable data resulting from their own work or from that of their organizations. The authors are especially indebted to Gary Cole for his thorough reading of the manuscript and his subsequent useful suggestions. The authors gratefully acknowledge the information provided by John Slater of NASA Glenn Research Center concerning the implementation of reflection coefficients into the WIND code. Thanks are due to Anthony B. Opalski for the contribution of some fine graphics.

References

[1] Cole, G. L., Melcher, K., Chicatelli, A. K., Hartley, T. T., and Chung, J. K., "Computational Methods for HSCT-Inlet Controls/CFD Interdisciplinary Research," AIAA Paper 94-3209, June 1994.

[2] Chung, J. K., "Numerical Simulation of a Mixed-Compression Supersonic Inlet Flow," AIAA Paper 94-0583, Jan. 1994.

[3]Chung, J. K., and Cole, G. L., "Comparison of Compressor Face Boundary Conditions for Unsteady CFD Simulations of Supersonic Inlets," AIAA Paper 95-2627, July 1995.

[4]Mayer, D. W., and Paynter, G. C., "Prediction of Supersonic Inlet Unstart Caused by Freestream Disturbances," *AIAA Journal*, Vol. 33, No. 2, 1995, pp. 266–276.

[5]Decher, R., Mayer, D. W., and Paynter, G. C., "On Supersonic Inlet-Engine Stability," AIAA Paper 94-3371, June 1994.

[6]Mayer, D. W., and Paynter, G. C., "Boundary Conditions for Unsteady Supersonic Inlet Analyses," *AIAA Journal*, Vol. 32, No. 6, 1994, pp. 1200–1206.

[7]Clark, L. T., "Dynamic Response Characteristics of a Mixed Compression Supersonic Inlet as a Part of a Larger System," AIAA Paper 95-0036, Jan. 1995.

[8]Atassi, H. M., "Unsteady Aerodynamics of Vortical Flows: Early and Recent Developments," *Advanced Series on Fluid Mechanics*, edited by K. Y. Fung, Aerodynamics and Aeroacoustics, World Scientific, Singapore, 1994, pp. 121–171.

[9]Kaji, S., and Okazaki, T., "Propagation of Sound Waves Through a Blade Row. Part I, Analysis based on the Semi-Actuator Disk Theory," *Journal of Sound and Vibration*, Vol. 11, No. 3, 1970, pp. 339–352.

[10]Kaji, S., and Okazaki, T., "Propagation of Sound Waves Through a Blade Row. Part II, Analysis Based on the Acceleration Potential Method," *Journal of Sound and Vibration*, Vol. 11, No. 3, 1970, pp. 355–375.

[11]Mani, R., and Horvay, G., "Sound Transmission Through Blade Rows," *Journal of Sound and Vibration*, Vol. 12, No. 1, 1970, pp. 59–83.

[12]Amiet, R. K., "Transmission and Reflection of Sound by a Blade Row," AIAA Paper 71-181, Jan. 1971.

[13]Cumpsty, N. A., and Marble, F. E., "The Interaction of Entropy Fluctuations with Turbine Blade Rows; A Mechanism of Turbojet Engine Noise," *Proceedings of the Royal Society of London, Series A: Mathematical and Physical Sciences*, Vol. 357, 1977, pp. 323–344.

[14]Paynter, G. C., Clark, L. T., and Cole, G. L., "Modeling the Response from a Cascade to an Upstream Acoustic Disturbance," *AIAA Journal*, Vol. 38, No. 8, 2000, pp. 434–440.

[15]Paynter, G. C., "Modeling the Response from a Cascade to an Upstream Convective Velocity Disturbance," AIAA Paper 98-3570, July 1998.

[16]Sajben, M., "Prediction of Acoustic and Entropy Pulses Created in Flow Systems by Sudden Additions of Mass, Momentum and Energy," AIAA Paper 99-0743, Jan. 1999.

[17]Sajben, M., "Prediction of Acoustic, Vorticity and Entropy Waves Generated by Short-Duration Acoustic Pulses Incident on a Blade Row," American Society of Mechanical Engineers, ASME Paper 99-GT-148, June 1999.

[18]Sajben, M., "Acoustic, Vorticity and Entropy Waves Created by Acoustic Pulses Incident on a Moving Blade Row," *Proceedings of the Fourteenth International Symposium on Airbreathing Engines (ISABE)*, Paper IS-088, 5–10, Sept. 1999.

[19]Paynter, G. C., "Response of a Two-Dimensional Cascade to an Upstream Disturbance," *AIAA Journal*, Vol. 35, No. 3, 1997, pp. 434–440.

[20]Suresh, A., Townsend, S. E., Cole, G. L., Slater, J. W., and Chima, R., Analysis of Inlet-Compressor Acoustic Interaction Using Coupled CFD Codes," AIAA Paper 99-0749, Jan. 1999.

[21]Suresh, A., and Cole, L., "Unsteady Analysis of Inlet–Compressor Acoustic Interactions Using Coupled 3D and 1D CFD Codes," NASA TM-2000-210247, Sept. 2000.

[22]Peacock, R. E., "An Experimental Study of Pulsating Flow in a Three-stage Axial-Flow Compressor," *Proceedings of the Winter Annual Meeting*, American Society of Mechanical Engineers, San Francisco, Dec. 1978, pp. 185–191.

[23]Das, D. K., "Effects of Inlet Pressure Fluctuations on Axial Flow Compressors," *Journal of Propulsion and Power*, Vol. 5, No. 1, 1989, pp. 72–82.

[24]Sajben, M., and Freund, D. D., "Experimental Exploration of Compressor-Face Boundary Conditions for Unsteady Inlet Flow Computations," AIAA Paper 95-2886, July 1995.

[25]Freund, D., and Sajben, M., "Compressor-Face Boundary Condition Experiment: Generation of Acoustic Pulses in Annular Ducts," AIAA Paper 96-2657, July 1996.

[26]Freund, D., and Sajben, M., "Experimental Investigation of Outflow Boundary Conditions Used in Unsteady Inlet Flow Computations," AIAA Paper 97-0610, Jan. 1997.

[27]Freund, D. D., and Sajben, M., "Reflection of Large Amplitude Acoustic Pulses from an Axial Flow Compressor," AIAA Paper 97-2879, July 1997.

[28]Sajben, M., and Freund, D. D., "Unsteady Inlet/Compressor Interaction Experiment to Support the Modeling of Compressor-Face Boundary Conditions," *Proceedings of the 8th International Symposium of Unsteady Aerodynamics and Aeroelasticity in Turbomachines*, Kluwer Academic, Norwell, MA, 1998, PP. 287–300.

[29]Freund, D., and Sajben, M., "Experiment to Support the Formulation and Validation of, Compressor-Face Boundary Conditions," *Journal of Propulsion and Power*, Vol. 16, No. 3, 2000, pp. 406–414.

[30]Kinsler, L. E., Frey, R. R., Coppens, A. B., and Sanders, J. V., *Fundamentals of Acoustics*, Wiley, New York, 1982, pp. 124, 125, 235.

[31]Rogers, T., "Ramjet Inlet/Combustor Pulsations Study," U.S. Naval Weapons Center, Silver Spring, MD, Rep. TP 6053, Jan. 1980, p. 149.

[32]Britsch, W. R., Osborn, W. M., and Laessig, M. R., "Effects of Diffusion Factor, Aspect Ratio, and Solidity on Overall Performance of 14 Compressor Middle Stages," NASA TP 1523, 1979.

[33]Slater, J. W., and Paynter, G. C., "Implementation of a Compressor Face Boundary Condition Based on Small Disturbances," American Society of Mechanical Engineers, ASME Paper 2000-GT-0005, May 2000.